Supporting Information for:

Syringe-Injectable Electronics with a Plug-and-Play Input/Output Interface

Thomas G. Schuhmann, Jr., [†] *Jun Yao,* [‡] *Guosong Hong,* [‡] *Tian-Ming Fu,* [‡] *and Charles M. Lieber**[†,‡]

†John A. Paulson School of Engineering and Applied Sciences and ‡Department of Chemistry and Chemical Biology, Harvard University, Cambridge, Massachusetts 02138, United States

Corresponding Author.

*E-mail: cml@cmliris.harvard.edu

This file includes:

Materials and Methods

Overall Design of Plug-and-Play Mesh Electronics

The design of plug-and-play mesh electronics' ultra-flexible device region is similar to previous reports.[1-3] Key parameters of the mesh (Figure 1) are: overall mesh width W = 2.2 mm, widths of longitudinal elements, w_1 = 20 μm, widths of transverse elements, w_2 = 10 μm, angle between longitudinal and transverse elements, α = 45°, spacing of longitudinal elements, L_1 = 333 μm, spacing of transverse elements, L_2 = 125 μm, metal interconnect line width, w_m = 4 μm, and total channel count N = 32. There are 19 longitudinal elements in a single mesh, with most carrying two interconnect lines with a pitch of 8 μm. Metal recording devices were located on both longitudinal and transverse elements (i.e., at midpoints between two adjacent transverse and longitudinal elements, respectively) as shown in Figure 1A, B (panel, i). Silicon nanowire field-effect transistor (NW-FET) based meshes had a similar design (Figure S1) with the following changes: The 19 longitudinal elements each has a single w_m = 10 μm metal interconnect that terminates at one of 19 independent I/O pads with 12 NW-FET drain channels, 3 common NW-FET source channels, and 4 Pt electrode channels. A schematic and dark-field microscopy image of one NW-FET in the mesh are shown in Figure S1. The ultra-flexible mesh region is ca. 1.3 cm long, which enables this portion to be injected into deep brain regions of mice and exit the skull similar to our previous studies.[1-3] After this mesh region the structure transitions to a flexible nonmesh stem region (Figure 1A, ii; 1B, ii). The stem is 300 μm wide, extends ca. 9 mm to the first I/O pad, and carries metal interconnects of width 4 μm with a pitch of 9 μm. Last, the uniform stem transitions to the foldable mesh I/O pads (Figure 1A, iii; 1B, iii). These pads have a mesh design with total width of 0.5 mm, length of 0.4 mm, pad pitch, p = 0.5 mm, width of longitudinal elements, 10 μm, width of transverse elements, 10 μm, metal conductor width of 6 μm, longitudinal and transverse element spacings, 50 μm, and 45° angle between longitudinal and transverse elements. Pads adjacent to a region of the stem unoccupied by interconnects extend their conductor onto this region of the stem, yielding the largest pad a width of 0.8 mm (0.5 mm from foldable mesh pad plus 0.3 mm on the stem) at the end distal to the mesh recording devices.

Fabrication of Mesh Electronics Containing Pt Electrodes

Fabrication of syringe-injectable mesh electronics has been reported previously,[1] with key steps as follows: (*i*) A sacrificial layer of 100 nm Ni was thermally evaporated (Sharon Vacuum, Brockton, MA) onto a pre-cleaned Si wafer (n-type 0.005 Ω·cm, 600 nm thermal oxide, Nova Electronic Materials, Flower Mount, TX). (*ii*) SU-8 negative photoresist (SU-8 2000.5; MicroChem Corp., Newton, MA) was spin-coated onto the Si wafer at 4000 rpm for an approximate thickness of 500 nm. It was pre-baked for 1 min at 65 °C and 1 min at 95 °C before photolithography (PL) patterning (MA6 mask aligner, Karl Suss Microtec AG, Garching, Germany) at an i-line dose of 100 mJ/cm^2 to define the bottom polymer mesh layer. (*iii*) The exposed SU-8 was post-baked for 1 min at 65 °C and 1 min at 95 °C before being developed (SU-8 Developer, MicroChem Corp., Newton, MA) for 2 min, rinsed in isopropyl alcohol, and hard-baked at 180 °C for 1 hour. (*iv*) The wafer was spin-coated at 4000 rpm with LOR 3A lift-off resist (MicroChem Corp., Newton, MA) and baked for 5 min at 180 °C, then spin-coated at 4000 rpm with Shipley 1813 positive photoresist (Microposit, The Dow Chemical Company, Marlborough, MA) and baked at 115 °C for 1 min. It was PL-patterned to define the metal interconnects at an h-line dose of 75 mJ/cm^2 followed by development (MF-CD-26, Microposit, The Dow Chemical Company, Marlborough, MA) for 1 min and rinsing in deionized (DI) water. (*v*) A 3 nm layer of Cr and 80 nm layer of Au were deposited by electron-beam evaporation (Denton Vacuum, Moorestown, NJ). Extraneous metal was removed in a lift-off process in solvent (Remover PG, MicroChem Corp., Newton, MA) heated to 80 °C. (*vi*) Steps *iv* and *v* were repeated to define 20 μm diameter Pt recording electrodes (3 nm Cr and 50 nm Pt). (*vii*) Steps *ii* and *iii* were repeated to define the top mesh polymer layer. (*viii*) Completed wafers were immersed in Ni etchant solution (40% $FeCl_3$:39% HCl:H_2O = 1:1:20) to dissolve the sacrificial Ni layer and release the mesh electronic probes from the wafer. Released mesh electronics were rinsed 3 times in DI water and transferred to 1X phosphate buffered saline (PBS) before injection.

Growth of Silicon Nanowires

Si NWs were grown in a home-built chemical vapor deposition (CVD) system using the nanocluster catalyzed vapor-liquid-solid (VLS) process.[4] Specific growth conditions were 50 nm diameter Au nanoparticles (Ted Pella Inc., Redding, CA) with gas flow rates of 2.5 sccm silane, 3 sccm diborane (100 ppm in He), and 60 sccm hydrogen carrier with growth temperature and

total pressure of 450°C and 40 Torr, respectively. The growth time of 1 hour yielded NWs with lengths of ca. 50 μm and a Si:B ratio of 4000:1.

Fabrication of Mesh Electronics Containing Nanowire Field-Effect Transistors

Meshes containing Si NW-FETs were fabricated the same as above for steps *i–iii.* (*iv*) NWs were contact printed from their growth substrates onto functionalized SiO_2.[5] They were then spin-coated with poly(methyl methacrylate) (950 PMMA C5, MicroChem Corp., Newton, MA) and transferred to the device region of the mesh electronics wafer.[6, 7] The PMMA was dissolved in acetone, leaving behind only NWs. Note that the number of nanowires per device was estimated to vary from 1 to 5. (*v*) The wafer was spin-coated at 4000 rpm with LOR 3A lift-off resist and baked for 5 min at 180 °C, then spin-coated at 4000 rpm with Shipley 1813 positive photoresist and baked at 115 °C for 1 min. It was patterned by PL to define the NW contacts and metal interconnects at an h-line dose of 75 mJ/cm^2 followed by development in MF-CD-26 for 1 min and rinsing in DI water. (*vi*) The wafer was immersed in 7:1 buffered oxide etch (BOE; Transene Company, Inc., Danvers, MA) for 5 sec followed by 10 sec rinse in DI water. Immediately after, a 3 nm film of Cr and 80 nm film of Au were deposited by thermal evaporation. Extraneous metal was removed in a lift-off process in Remover PG heated to 80 °C. (*vii*) Step *v* was repeated to mask NWs in desired locations within the mesh. Excess NWs were removed with reactive ion etching (RIE; STS MPX/LPX RIE system, SPP, Newport, United Kingdom). Masking resist was removed in Remover PG. (*viii*) Steps *ii* and *iii* were repeated to define the top mesh polymer layer. (*ix*) Completed wafers were immersed in Ni etchant solution to dissolve the sacrificial Ni layer and release the mesh electronic probes from the wafer. Released mesh electronics were rinsed 3 times in DI water and transferred to 1X PBS before injection.

Controlled Injection into Hydrogel and Clamp-Connect I/O Interfacing

Loading Mesh Electronics into Capillary Tubes.

Needles used for injection experiments were glass capillary tubes (Drummond Scientific Co., Broomall, PA.) with an inner diameter (I.D.) of 400 μm and outer diameter (O.D.) of 650 μm. Glass capillary tubes were inserted into a micropipette holder (Q series holder, Harvard Apparatus, Holliston, MA), which was connected to a 1-mL syringe (NORM-JECT®, Henke Sass Wolf, Tuttlingen, Germany) through a polyethylene intrademic catheter tubing (I.D. 1.19

mm, O.D. 1.70 mm, Becton Dickinson and Company, Franklin Lakes, NJ). With the mesh electronics suspended in a 100 mL beaker of 1X PBS, the capillary needle was positioned close to the I/O end of the structure (identified easily by visual inspection), and then the syringe was pulled manually to draw the mesh electronics from the solution into the glass capillary tube. The mesh electronics' position within the needle was adjusted by pushing/pulling the syringe while immersed in solution until the mesh electronics was located with the ultra-flexible device region just inside the bottom of the capillary needle (also easily identified by visual inspection). This configuration minimizes the volume of solution injected while ensuring the device region is injected first and the I/O pads last.

Preparation of Hydrogel.

0.5 g agarose (SeaPlaque® Lonza Group Ltd., Basel, Switzerland) was mixed with 100 mL DI water in a glass beaker. The beaker was covered with aluminum foil (Reynolds Wrap® Reynolds Consumer Products, Lake Forest, Illinois) to prevent evaporation and heated to boiling on a hot plate while mixed with a magnetic stir rod. Once the solution became transparent, the hot plate was switched off and the solution was allowed to cool to room temperature. The resulting hydrogel has a final mass concentration ca. 0.5% and mechanical properties similar to those of dense brain tissue.[3, 8, 9]

Controlled Injection of Mesh Electronics into Hydrogel.

Mesh electronics were injected by the field of view (FoV) method, described previously.[3] Briefly, the 0.5% agarose hydrogel was poured into a cuvette to cool. A glass capillary tube loaded with mesh electronics was inserted into a micropipette holder, which was connected to a 5 mL syringe (Becton Dickinson and Company, Franklin Lakes, NJ) via polyethylene intrademic catheter tubing (I.D. 1.19 mm, O.D. 1.70 mm). The 5 mL syringe was filled with 1X PBS and driven by a syringe pump (PHD 2000, Harvard Apparatus, Holliston, MA). The micropipette holder was fixed to a motorized stereotaxic stage (860A motorizer and 460A linear stage, Newport Corporation, Irvine, CA) for precise control of injection depth and rate. The stereotaxic stage was used to lower the end of the glass capillary tube into the hydrogel-filled cuvette to its target depth. Controlled injection was achieved by focusing an eyepiece camera (DCC1240C, Thorlabs Inc., Newton, NJ) on the top of the mesh electronics (I/O pad region) and matching the

stereotaxic retraction rate of the glass capillary tube to the rate of mesh electronics injection due to fluid flow from the syringe pump. Typical injection flow rates were 10–50 mL/h with total injection volumes less than 50 μL per 4 mm length of injected mesh.

Clamp-Connect I/O Interfacing to Mesh Electronics.

Once mesh electronics were injected to the desired depth, the glass capillary tube was repositioned using the stereotaxic stage to a clamping substrate which had been adhered to the top of the cuvette. We found that two pieces of dicing tape (thick clear low tack roll 24353, Semiconductor Equipment Corp., Moorpark, CA) adhered together (adhesive sides in) worked well as a clamping substrate. The I/O pads of mesh electronics were ejected by resuming fluid flow until all I/O pads were on the tape. The I/O stem region was flipped with tweezers so the I/O pad conducting sides faced up, if necessary, and was smoothly bent to a 90° angle as near to the first I/O pad as possible. The I/O pads were rinsed by pipetting drops of DI water over them slowly; this same process was sometimes used to unfold mesh I/O pads which occasionally did not fully extend upon ejection from the capillary tube. The I/O pads and stem were dried in place with compressed air. The dicing tape was subsequently cut with scissors to a distance of ca. 0.5 mm from the I/O pad edges; this distance was selected to align the I/O pads with the zero insertion force (ZIF; Hirose connector FH12A-32S-0.5SH(55), HIROSE Electric, Downers Grove, IL) connector pins when the dicing tape has been inserted as far as possible inside the connector. The trimmed tape and I/O pads were then inserted into the ZIF connector which had been mounted on a custom-made printed circuit board (PCB; Advanced Circuits, Aurora, CO) shown in Figure S2. Once fully inserted, the ZIF connector latch was secured shut to make electrical contact with the mesh I/O pads. Successful connection was checked with an ohmmeter or by interfacing to peripheral electronics; in case of misalignment, the tape and pads could be removed from the connector and reinserted after adjustment.

Electrical Characterization of Plug-and-Play Mesh Electronics

Four-Point Probe Measurements.

A large-area (1.5 cm x 1.5 cm) mesh I/O pad otherwise identical to those used on plug-and-play mesh electronics was fabricated and clamp-connected on dicing tape using the procedures described above (Figure S4, A). The circuit resistance (Figure S4, B) was measured with a home-

built four-point probe setup consisting of a precision current source (Keithley 6220, Tektronix, Inc., Beaverton, OR) and voltmeter (Analog Discovery 2, Digilent Inc., Pullman, WA). The lateral resistance R_L through the mesh I/O pad is a function of distance, while the ZIF-to-mesh contact resistance R_C and wire resistance R_W (due to a flat flexible cable, two interfacing PCBs, and pin socket wires) are fixed. A plot of resistance vs. distance, therefore, reveals a linear function with y-intercept equal to twice $R_C + R_W$ (Figure 3A). We measured $R_W = 0.26\ \Omega$ and the best-fit line's y-intercept was 6.43 Ω ($r^2 = 0.94$), yielding a typical contact resistance $R_C \approx 3\ \Omega$.

Electrode Impedance Characterization.

Mesh electronics containing 32 Pt electrodes of 20 μm diameter were injected in 1X PBS and clamp-connected on dicing tape with the PCB-mounted ZIF connector. They were interfaced through a flat flexible cable (FFC) and home-made PCB connected to an Intan RHD 2132 amplifier system (Intan Technologies LLC, Los Angeles, CA). Electrode interfacial impedance was measured at 1 kHz using the Intan system's built-in electrode impedance measurement function while the 1X PBS was grounded with a Au wire.

Frequency-Dependent Electrode Impedance Measurement.

Mesh electronics containing 32 Pt electrodes of 20 μm diameter were pipetted from DI water onto a glass slide. The mesh I/O pads were dried in place while the mesh device region was immersed in a drop of 1X PBS pipetted onto the slide. A home-built probe system consisting of precision probe positioners (DCM-210, Cascade Microtech, Beaverton, OR), a precision current amplifier (SIM918 precision current preamp and SIM900 mainframe, Stanford Research Systems, Sunnyvale, CA), and a digital network analyzer (Analog Discovery 2, Digilent Inc., Pullman, WA) was used to measure the impedance between individual electrode channels and a Au wire immersed in the 1X PBS. Impedance was measured in response to an applied 100 mV sinusoid swept from 10 Hz to 10 kHz.

Frequency-Dependent Inter-Channel Impedance Measurement.

Mesh electronics containing 32 Pt electrodes of 20 μm diameter were pipetted from DI water onto a glass slide. The entire mesh probe was dried in place before a ca. 5 mm diameter droplet of 1X PBS was pipetted over the stem interconnect region while the I/O pads and electrodes

remained dry. A home-built probe system consisting of precision probe positioners (DCM-210, Cascade Microtech, Beaverton, OR), a precision current amplifier (SIM918 precision current preamp and SIM900 mainframe, Stanford Research Systems, Sunnyvale, CA), and a digital network analyzer (Analog Discovery 2, Digilent Inc., Pullman, WA) was used to measure the impedance between adjacent channels of the mesh electronics. Impedance was measured for n = 16 adjacent channel pairs in response to an applied 100 mV sinusoid swept from 10 Hz to 10 kHz.

Nanowire Transistor Characterization.

Mesh electronics containing 12 NW-FETs were injected into 1X PBS and clamp-connected on dicing tape with the PCB-mounted ZIF connector. They were interfaced through a FFC and home-made PCB connected to a precision current amplifier (SIM918 precision current preamp and SIM900 mainframe, Stanford Research Systems, Sunnyvale, CA). The signals were digitized with a Digidata 1440A Digitizer (Molecular Devices, Sunnyvale, CA) and pCLAMP 10 data acquisition software (Molecular Devices, Sunnyvale, CA). Current-voltage (I-V) curves were measured by recording I_{DS} while grounding the 1X PBS with a Au wire and sweeping V_{DS} from -100 mV to +100 mV. Water gate responses were measured by applying 100 mV to V_{DS} while recording I_{DS} and sweeping the 1X PBS-immersed Au wire from -200 mV to + 200 mV. Time domain signals were post-processed in Python to extract I-V and water gate curves for each device.

***In Vivo* Injection and I/O Interfacing to Plug-and-Play Mesh Electronics**

Vertebrate Animal Subjects.

Vertebrate animal subjects used in this study were 6–8 week old adult (25-35 g) male C57BL/6J mice (Jackson Laboratory, Bar Harbor, ME). All procedures performed on the vertebrate animal subjects were approved by the Animal Care and Use Committee of Harvard University. The animal care and use programs at Harvard University meet the requirements of the Federal Law (89-544 and 91-579) and National Institutes of Health (NIH) regulations and are also accredited by the American Association for Accreditation of Laboratory Animal Care (AAALAC). Animals were fed with food and water *ad libitum* as appropriate and were group-housed on a 12 h/12 h light/dark cycle in the Harvard University Biology Research Infrastructure (BRI).

Injection of Mesh Electronics into Live Mice Brains.

In vivo injection of mesh electronics has been described previously.[1-3] Briefly, all metal tools in direct contact with the mice were autoclaved for 1 h and all plastic tools in direct contact with the mice were sterilized with 70% ethanol and rinsed with sterile DI water and sterile 1X PBS before use. Mesh electronic samples were sterilized with 70% ethanol, then rinsed with sterile DI water and transferred to sterile 1X PBS. Mice were anesthetized by intraperitoneal (IP) injection of a mixture of 75 mg/kg of ketamine (Patterson Veterinary Supply Inc., Chicago, IL) and 1 mg/kg dexdomitor (Orion Corporation, Espoo, Finland). Mice were placed on a heating pad (Harvard Apparatus, Holliston, MA) set to 37°C to maintain body temperature throughout surgery and recovery. Depth of anesthesia was monitored by pinching the mice's feet. In preparation for injection, a mouse was placed in the stereotaxic frame (Lab Standard Stereotaxic Instrument, Stoelting Co., Wood Dale, IL) with two ear bars and one nose clamp to fix the head in place. Hair removal lotion (Nair®, Church & Dwight, Ewing, NJ) was applied for depilation of the mouse head and iodophor was used to sterilize the depilated scalp skin. The scalp was resected from the center axis of the skull to expose a ca. 4 mm^2 section of the skull. Two 1 mm diameter burr holes were formed in opposite hemispheres of the skull using a dental drill (Micromotor with On/Off Pedal 110/220, Grobet USA, Carlstadt, NJ). The dura was carefully incised and resected, and sterile 1X PBS was swabbed on the surface of the brain to keep it moist throughout the surgery. The left burr hole was fitted with a sterilized 0-80 set screw (18-8 Stainless Steel Cup Point Set Screw; outer diameter: 0.060" or 1.52 mm, groove diameter: 0.045" or 1.14mm, length: 3/16" or 4.76 mm; McMaster-Carr Supply Company, Elmhurst, Illinois) to serve as the grounding/reference electrode. A piece of sterilized dicing tape (as prepared in "Clamp-Connect I/O Interfacing to Mesh Electronics") was adhered adjacent to the right burr hole with METABOND dental cement (Parkell Inc., Edgewood, New York) prior to injection to serve as a clamping substrate for the I/O pads. The same injection process as described in "Controlled Injection of Mesh Electronics into Hydrogel" was used for injection of mesh electronics into the live mouse brain. The stereotaxic coordinates used for injection were: anteroposterior, 0.98 mm; mediolateral, 0.95 mm; dorsoventral, 4 mm. The recording electrodes are distributed over a depth of 2 mm within the mesh, placing them approximately within the caudoputamen region of the brain. Typical solution volumes injected into the brain per 4 mm length of mesh were <50 μL.

I/O Interfacing to In Vivo Mesh Electronics.

After injection in the brain, the capillary tube was guided to the dicing tape using the stereotaxic stage, where fluid flow was resumed to eject the mesh I/O pads. Clamp-connection to the dicing tape cemented to the mouse skull was carried out with a sterilized PCB connector using the procedure described in "Clamp-Connect I/O Interfacing to Mesh Electronics." The PCB was then flipped (ZIF components facing the mouse) and its end nearest to the burr hole was cemented to the exposed skull. Additional dental cement was used to secure the latch of the ZIF connector clamped to the mesh I/O pads, protect exposed areas of the mesh electronics and dicing tape, and protect the scalp, with care taken to ensure access for an FFC to be inserted in the ZIF connector on the other end of the PCB. Acute recordings were acquired approximately 1 hr after injection. Mesh electronics were interfaced via an FFC inserted into the PCB cemented to the mouse skull, which in turn connected to a home-made PCB with leads to the Intan RHD 2132 amplifier system. *In vivo* recording data was acquired at a 20 kHz sampling rate with a 60 Hz notch filter applied at the time of acquisition while the 0-80 set screw was used as reference. Mice were held in a Tailveiner restrainer (Braintree Scientific, LLC, Braintree, MA) throughout recording. Mice used only for acute recordings were euthanized following measurements via intraperitoneal injection of Euthasol at a dose of 270 mg/kg body weight.

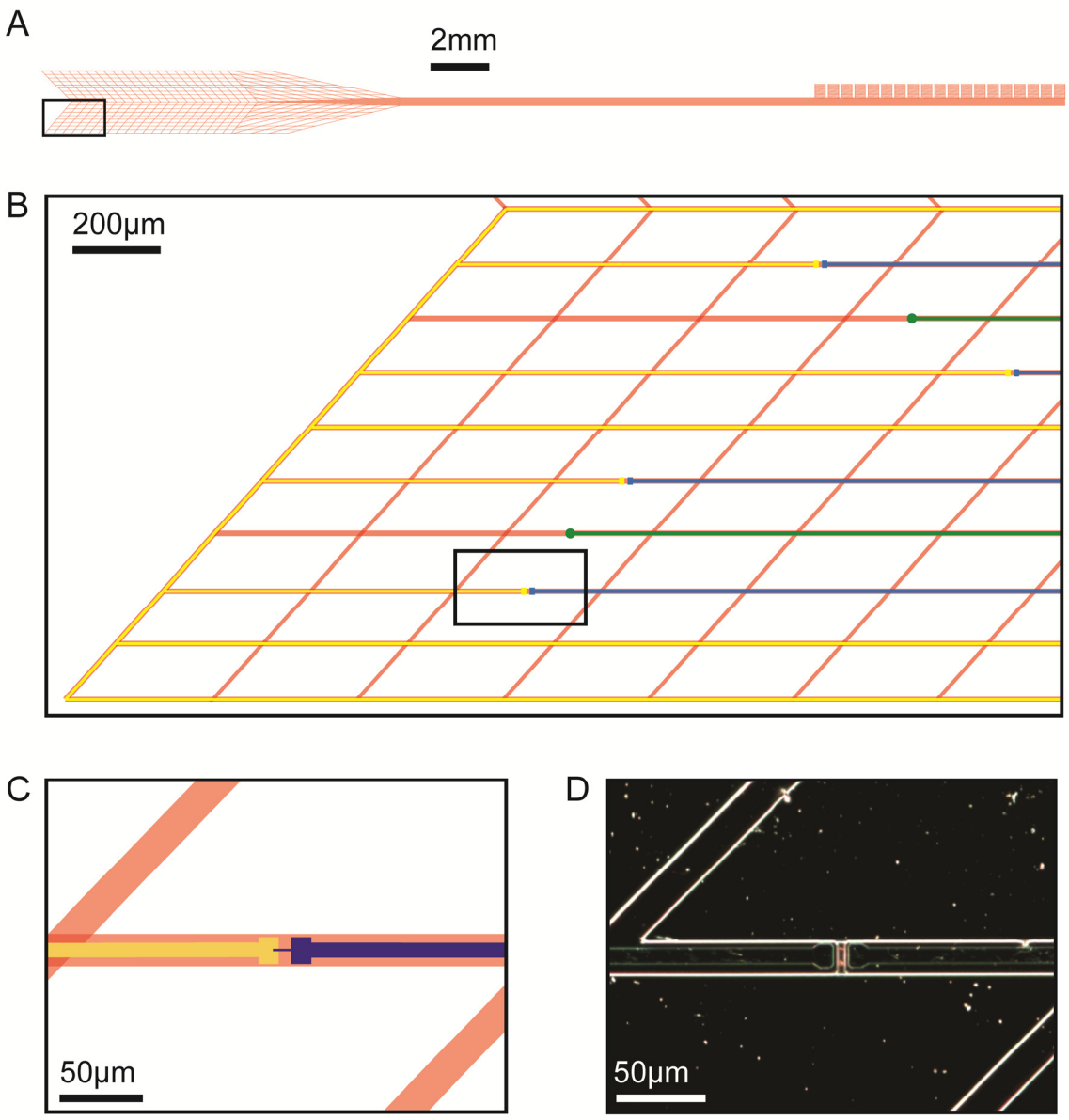

Figure S1. Design of plug-and-play mesh electronics with NW-FETs. (A) Schematic overview of plug-and-play mesh electronics containing 12 NW-FETs and 4 Pt recording electrodes. (B) Magnified view of the boxed region in (A) showing the layout of NW-FETs and electrodes within one section of the mesh device region. NW-FETs are powered through a common source (conductors colored in yellow) accessible via 3 separate I/O pads. Each of the individually addressed NW-FET drains (conductors colored in blue) has a dedicated interfacing I/O pad, as does each of the Pt recording electrodes (conductors colored in green). (C) Magnified view of the boxed region in (B) detailing an individual NW-FET device. The source electrode (yellow) and drain electrode (blue) is spanned by a NW channel (black). (D) Dark-field optical

microscope image of a NW-FET as designed in (C), which contains ca. two Si NWs highlighted by their light scattering, which makes the NWs appear as short orange-red horizontal lines located in the center of the image between the source and drain electrodes.

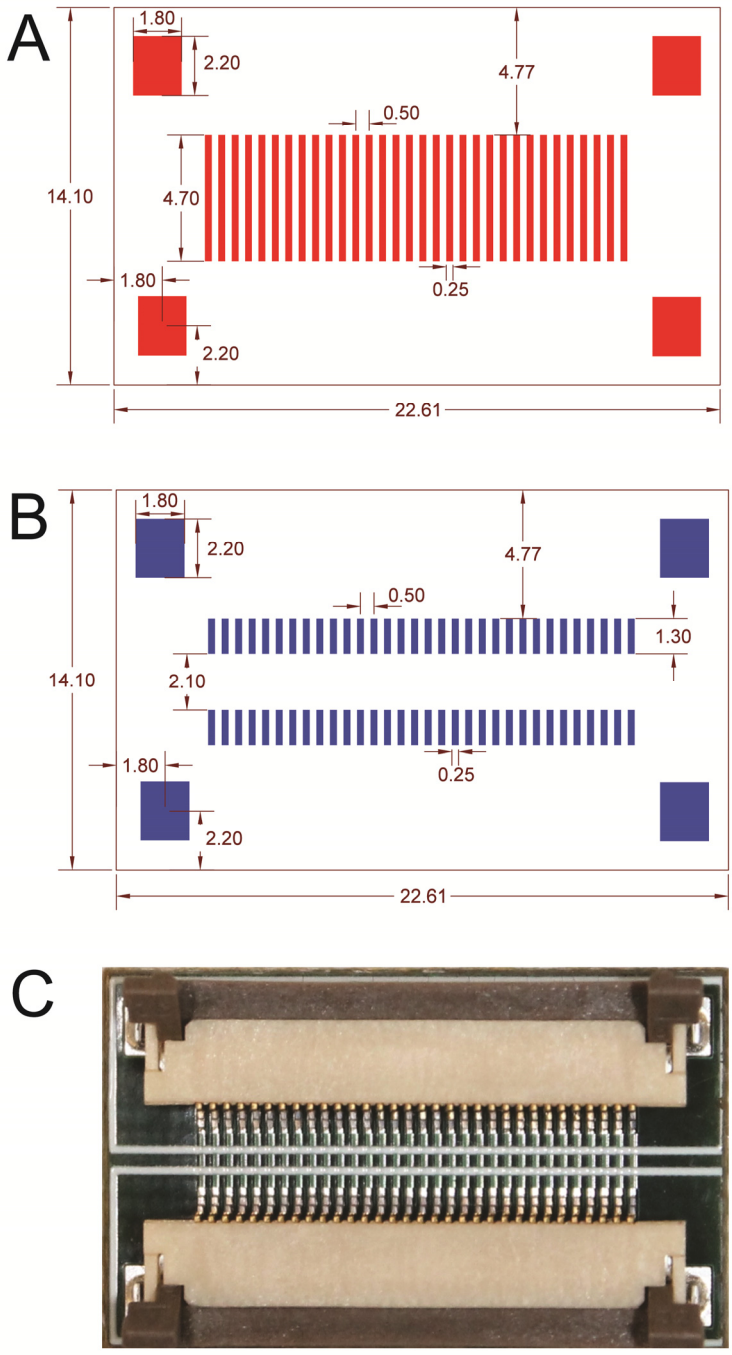

Figure S2. Custom PCB for clamp-connection to mesh electronics. (A) Schematic of the copper routing on a custom-made PCB used to interface with plug-and-play mesh electronics (units in mm). (B) Schematic of the solder mask used to define component landing pads on the custom PCB (units in mm). (C) Photograph of the PCB after manufacturing. The PCB contains two identical ZIF connectors, with one used to clamp the mesh I/O pads and the other to interface with an FFC leading to peripheral electronics. The size is the same as in (A) and (B) schematics, and the final assembled weight is 1.54 g.

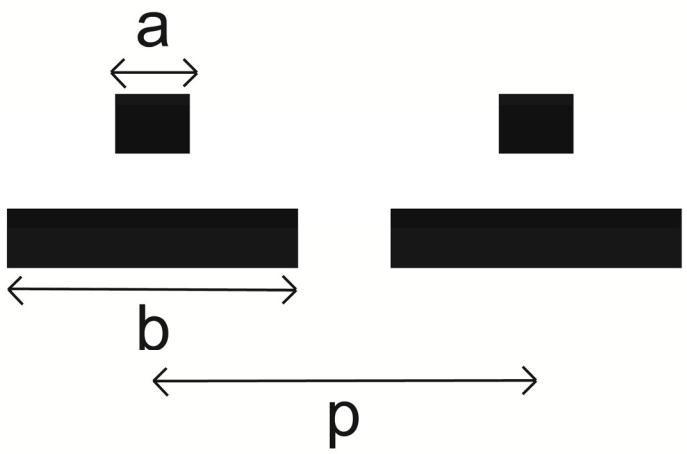

Figure S3. Optimum geometry for I/O pad design. For a ZIF connector with pin width *a* and pitch *p*, the optimum selection of mating pad width *b* is $b = p - a$.[10] For a larger choice of *b*, it becomes likely blind insertion will result in shorting adjacent channels; for smaller, it becomes likely channels will not be connected at all. When $b = p - a$, 1:1 interfacing occurs with nearly 100% yield.

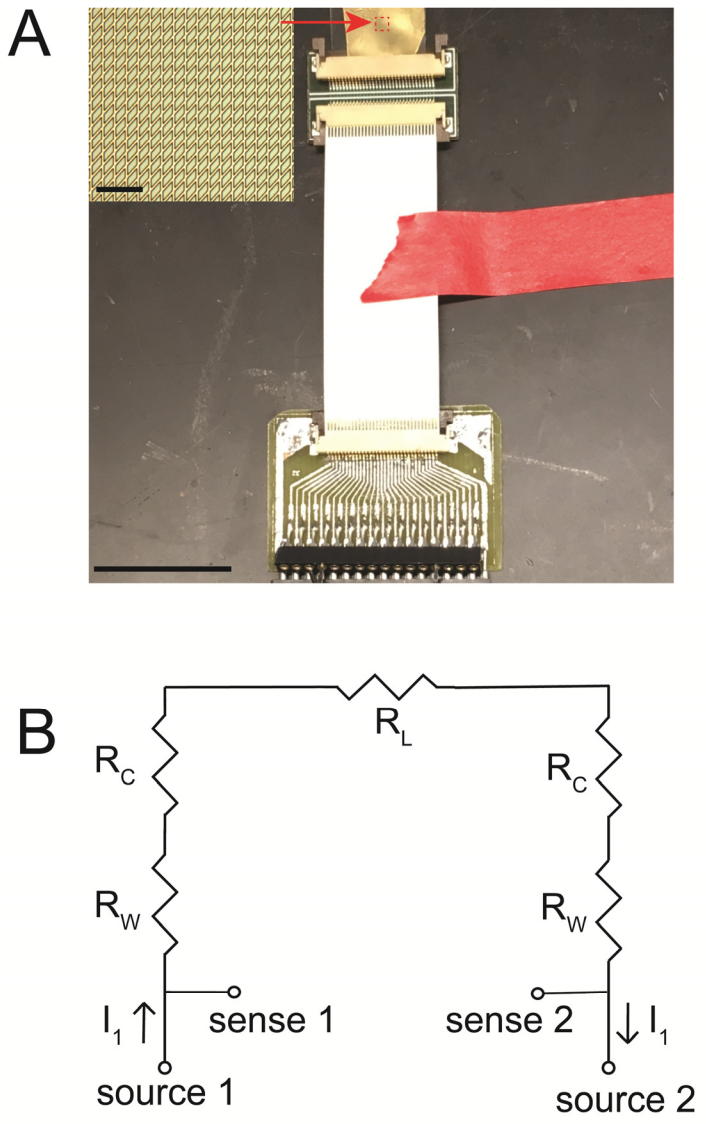

Figure S4. Four-point probe measurements of contact resistance. (A) Photograph of the experimental setup used for four-point probe contact resistance measurements. The large-area mesh I/O pad (red arrow) is clamped in a PCB at the top of the image. Each channel is individually addressable through an FFC interfacing to another PCB with pin socket outputs to amplifier electronics. Scale bar is 2 cm. (inset) Optical microscopy image recorded from the region highlighted by the dashed box at tip of arrow in main image; scale bar is 200 μm. (B) Circuit diagram for four-point probe measurements. The lateral resistance R_L through the mesh is a linear function of distance (known from the ZIF connector pin pitch of 0.5 mm). It is in series with a fixed resistance contributed by the ZIF-mesh contact resistance R_C plus a wire resistance R_W contributed by the interfacing wire, PCBs, and FFC. In a linear plot of resistance vs. distance, the y-intercept is approximately twice $R_C + R_W$.

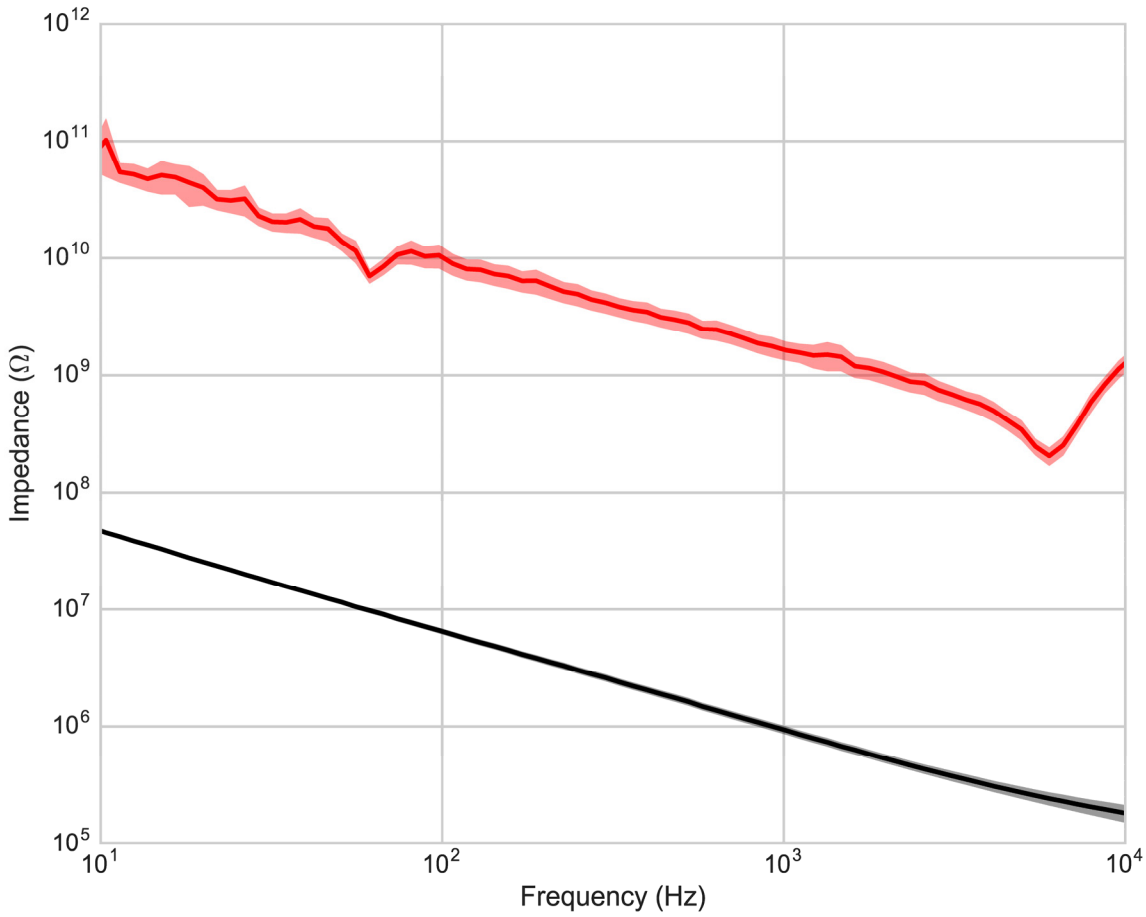

Figure S5. Frequency-dependent impedance of plug-and-play mesh electronics channels. (Black) Interfacial impedance of 20 μm diameter Pt electrodes in 1X PBS. Impedance was measured at 100 mV between individual electrodes and a Au wire inserted in the 1X PBS. The plotted data are the mean (black line) ± standard error of mean (gray outline) for n = 16 electrodes. (Red) Impedance between adjacent channels in mesh electronics. Impedance was measured at 100 mV with the stem interconnects immersed in a drop of 1X PBS while the mesh I/O pads and recording electrodes were dry. The plotted data are the mean (red line) ± standard error of mean (light red outline) for n = 16 channel pairs.

Supplementary References

1. Liu, J.; Fu, T. M.; Cheng, Z.; Hong, G.; Zhou, T.; Jin, L.; Duvvuri, M.; Jiang, Z.; Kruskal, P.; Xie, C.; Suo, Z.; Fang, Y.; Lieber, C. M. *Nat. Nanotechnol.* **2015,** *10*, 629-636.
2. Fu, T. M.; Hong, G.; Zhou, T.; Schuhmann, T. G.; Viveros, R. D.; Lieber, C. M. *Nat. Methods* **2016,** *13*, 875-882.
3. Hong, G.; Fu, T. M.; Zhou, T.; Schuhmann, T. G.; Huang, J.; Lieber, C. M. *Nano Lett.* **2015,** *15*, 6979-6984.
4. Patolsky, F.; Zheng, G.; Lieber, C. M. *Nat. Protoc.* **2006,** *1*, 1711-1724.
5. Yao, J.; Yan, H.; Lieber, C. M. *Nat. Nanotechnol.* **2013,** *8*, 329-335.
6. Reina, A.; Jia, X.; Ho, J.; Nezich, D.; Son, H.; Bulovic, V.; Dresselhaus, M. S.; Kong, J. *Nano Lett.* **2009,** *9*, 30-35.
7. Jiao, L.; Fan, B.; Xian, X.; Wu, Z.; Zhang, J.; Liu, Z. *J. Am. Chem. Soc.* **2008,** *130*, 12612-12613.
8. Chen, Z. J.; Gillies, G. T.; Broaddus, W. C.; Prabhu, S. S.; Fillmore, H.; Mitchell, R. M.; Corwin, F. D.; Fatouros, P. P. *J. Neurosurg.* **2004,** *101*, 314-322.
9. Deepthi, R.; Bhargavi, R.; Jagadeesh, K.; Vijaya, M.; Signal, B.; Processing, I.; Author, C. *SAS Tech J.* **2010,** *9*, 27-30.
10. Gillett, J. B.; Washo, B. D. Connector and Cable Packaging. In *Microelectronics Packaging Handbook*; Tummala, R. R., Rymaszewski, E. J., Eds.; Von Nostrand Reinhold: New York, 1989; pp 955-1020.